COMPUTATION AND USE OF THE REFLECTIVITY AT 3.75 μM FROM AVHRR THERMAL CHANNELS.

J.C. ROGER and E. F. VERMOTE
NASA Goddard Space Flight Center - Code 923
Greenbelt, MD 20771, USA

ABSTRACT:

Global study of land surface properties uses AVHRR channels 1 and 2 but channel 3 may be of interest too but its use requires preprocessing. It consists of both a reflective part and an emissive part, the former can be derived from T_3, T_4 and T_5. Moreover, since the water vapor affects channel 3, its content is retrieved from the channel 4 and 5 using the Split Window Technique. A formula of reflective part retrieval at 3.75 μm is first tested in the case of sunglint observations where the emissivities of channels 4 and 5 can be set to the unity. In a second part of the formula is adapted and validated to land surface using the FIFE-87 data set. The last section is devoted to some preliminary applications of the reflectance at 3.75 μm to the studies of surface properties retrieval, aerosol retrieval over land and desertic aerosol retrieval.

KEY WORDS: Reflectivity at 3.75 μm, Water vapor retrieval, Thermal channels, AVHRR

1 - INTRODUCTION

For the last 25 years, data of the Earth-Atmosphere system has been continuously acquired from the Advanced Very High Resolution Radiometers (AVHRR) on-board NOAA polar orbiting satellites. Since the AVHRR carries visible, infrared and thermal bands, and since a complete coverage of the Earth is available twice daily with 2 resolutions (1 and 4 km), and from two platforms, the data represent a potentially valuable source of information. This allows for the first time a possible monitoring of the ocean, terrestrial and atmospheric processes at local and global scales.

Over ocean extensive uses have been done using channels 4 and 5 for the determination of the Sea Surface Temperature [Prabhakara et al., 1974; Mc Millin, 1975; for the first ones], or channel 1 for aerosol optical thickness retrieval [Rao et al., 1989]. Over land, the principal use of AVHRR has been to combine the channels 1 and 2 to derive the Normalized Difference Vegetation Index (NDVI) [Tucker et al, 1981; Gatlin et al., 1983; Justice et al., 1985] and the quantitative estimate of biomass production [Daughtry et al., 1983; Tucker et al, 1983 and 1985]. Channel 3 has been used to assess deforestation and biomass burning [Malingreau et al., 1989; Setzer, 1991]. In some recent papers, understanding of the signal measured by channels 4 and 5 over land has been demonstrated [Becker and Li, 1990; Kerr et al., 1992; Ottlé and Vidal-Madjar, 1992; Seguin et al., 1992]. The Challenge in using channel 3 is the decoupling between thermal emission and reflective properties of the target. It is tempting to try to combine the channels 4, 5 and 3 to derive quantitative estimate of the reflectance at 3.75μm. The use of the derived reflectance is important for AVHRR aerosol retrieval method over land, as shown by Vermote et al. (1993), but could be also interesting for sunglint correction over ocean, studies of bidirectionnal reflectances or desertics aerosol outbreaks.

In this paper, we try to validate a formula of reflectance at 3.75 μm based on the channels 3, 4 and 5, NDVI observations and MODTRAN simulations. Because channel 3 is sensitive to water vapor, the problem of water vapor retrieval, both over land and sea, is also examined using one year of SSM/I water vapor retrieval, AVHRR data and sunphotometer measurements. In a second part, we validate the formula in the case of sunglints observations where the emissivities of channels 4 and 5 can be set to 1.00. In a third part, the reflectance over land is retrieved and compared to indirect measurements performed during FIFE-87 experiment. In this case, the emissivities of the channels 4 and 5 are no longer equal to 1.00 but can be estimated using NDVI. The latest part presents applications of the reflectance formula for studies of surface properties retrieval, aerosol retrieval over land and desertic aerosol studies.

2 - WATER VAPOR RETRIEVAL FROM THERMAL CHANNELS

In channel 3 the effect of the water vapor should be accounted for. As it varies strongly with time and space, it is important to get the water vapor content at the time and location of the AVHRR observed radiances. Several published studies have used T_4-T_5 (Split Window Technique) for the retrieval of the amount of water vapor in the atmosphere [Prabhakara et al., 1974; Dalu, 1986; Schluessel, 1989; Justice et al., 1991]. We tried to retrieve and to improve the relation between water vapor content and T_4-T_5 both over ocean and land.

2.1. Retrieval of water vapor over sea.

Over sea, we used one year of SSM/I and AVHRR data over the Pacific Ocean, to establish the relation. We assume that water vapor content is linearly proportional with T_4-T_5 [Dalu, 1986]:

$$U_{h2o} = A(\theta).\ (T_4\text{-}T_5) \qquad (01)$$

A plot of SSM/I water vapor content versus nadir measurements of T_4-T_5 is given Figure 1a. The coefficient A can be deduced: $A(0°)=1.98 \pm 0.5$ g/cm^2/°k. For a viewing angle θ=60°, this coefficient becomes, Figure 1-b, $A(60°)=1.53 \pm 0.5$ g/cm^2/°K.

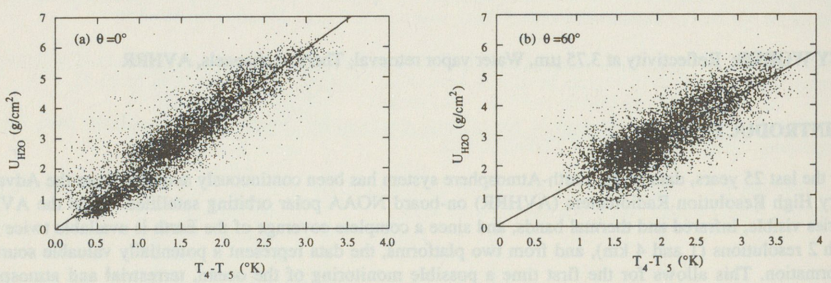

Figures 1: Plot of U_{h2o} from SSM/I versus (T4-T5) for 2 zenith angles (a) 0° and (b) 60°.

The angular dependency for some values of cos(θ) is shown in Figure 2. The retrieved results are then compared to theoretical computations. Defining 36 different atmospheres with a water vapor content ranging from 0 to 6.5 g/cm^2, we computed with Lowtran7 the coefficient A for different angles. These computations confirm the angular dependency of coefficient A that does not follow a cos(θ) law [Dalu, 1986].

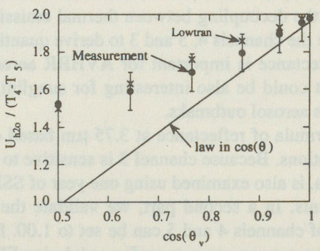

Figure 2: Angular dependency of A(θ) determined over sea both by the measurement and by the computations. Also reported, the law in cos(θ)

2.2. Retrieval of water vapor over land.

Over Land, to retrieve the relation we used AVHRR data and the sunphotometer measurements performed during the SCAR-A experiment which has been conducted in the Eastern US coast on July 1993. Figure 3 shows

that the coefficient A(0°) is now equal to 1.00 and does not depend of the viewing angle. This coefficient A is close to the result given by Justice et al. [1991] for a Sahelian environment.

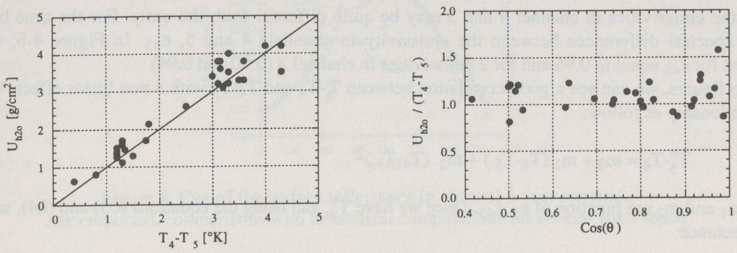

Figure 3: (a) Plot of U_{h2o} from Sunphotometer versus (T4-T5) over land for θ_v equal to 0°
(b) Angular dependency of A(θ) determined

3 - SURFACE REFLECTANCE IN CHANNEL 3

3.1. Formula of the surface reflectance.

The radiance in the channel 3 includes both the emissive part R_3^e and reflective part R_3^r of the surface and of the atmosphere. For a cloud free atmosphere the signal can be written as follow:

$$R_3 = R_3^e + R_3^r \tag{02}$$

with

$$R_3^r = \frac{1}{\Pi} \rho_3 E_s \cos(\theta_s) \tau_3(\theta_v) \tau_3(\theta_s) \tag{03}$$

where θ_s et θ_v are the solar and view zenith angles, τ the transmittance, ρ_3 the reflectivity of the surface at 3.75µm, E_s the incident solar radiance.
Using the Planck function, we can define the temperatures T_3 and T_3^e from R_3 and R_3^e, then the equation (02) becomes:

$$R_3 = B_3(T_3) = B_3(T_3^e) + R_3^r \tag{04}$$

In order to evaluate R_3^r, we need to determine the temperature due to emission T_3^e. To minimize the effects of variable atmosphere we use the relationship between T_3^e-T_4 and T_4-T_5. Using the 36 atmospheres described above, we compute T_3^e, T4 and T5 for view zenith angle from 0° to 50° and for 20 emissivities ranging 1.00 to 0.80 for channels 3, 4 and 5.

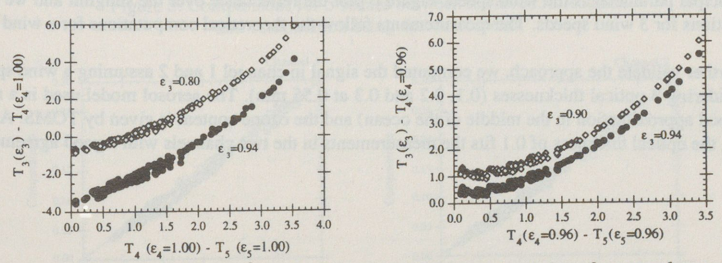

Figures 4: Comparisons between T_3-T_4 with T_4-T_5 from MODTRAN simulations for several case of ε_3 and ε_{45}
(a) Typical case of Sunglint ε_3=0.80 and 0.94, ε_{45}=1.00, (b) Case of vegetation ε_3=0.90 and 0.94, ε_{45}=0.96

Over sea, we can assume an emissivity in the channel 4 and 5 equals to the unity (Takashima and Takayama, 1981). Figure 4-a shows the result of the computation for a typical case of sunglint (emissivity ε_3 of 0.80 and 0.94).
Over land, the emissivities in channel 4 and 5 may be quite different from the unity. For the time being, we assume no spectral differences between the emissivity in channels 4 and 5, ε_{45}. In Figure 4-b, we show computations for ε_{45} equal to 0.96 and for 2 emissivities in channel 3 (0.90 and 0.94)
In these two figures, we can see a good correlation between T_3^e-T_4 and T_4-T_5 with a non linear effect. We then define a relationship as follow:

$$T_3^e - T_4 = m_0 + m_1.(T_4 - T_5) + m_2.(T_4 - T_5)^2 \qquad (05)$$

where m_0, m_1 and m_2 are function of ε_3, ε_{45}. Once we have T_3^e, and using the equations (03) and (04), we get the surface reflectance:

$$\rho_3 = \frac{\Pi\,[B_3(T_3) - B_3(T_3^e)]}{E_s \cos(\theta_s)\,\tau_3(\theta_v)\,\tau_3(\theta_s)} \qquad (06)$$

3.2. Validation over sea

Using ε_{45} equal to 1.00, we computed T_3 for 3 solar zenith angles (0°, 30° and 60°) and for the conditions described for our theoretical data set.
Figure 5 shows the theoretical retrieval of the surface reflectances in the case of sunglint observations. The observed discrepancy is less than 10% in RMS for a solar zenith angle of 60° and decreases to less than 5% for an angle of 0°.

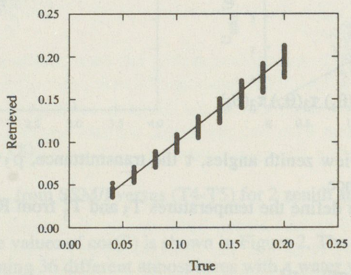

Figure 5: Theoretical retrieval of surface reflectances in channel 3 using (06) for sunglint cases.

We tested the formula with 5 AVHRR scenes over Pacific Ocean between 1985 and 1990. First we computed images of the reflectance in channel 3 and then we compared with theoretical computations of sunglint using Cox and Munk parametrization [1954]. Except for desertic aerosols the effect of aerosols is very low in channel 3 and the principal parameter is the wind speed. Figure 6 plot the reflectance over the sunglint and we compare with computations for 3 wind speeds. The measurements follow the theoretical computations for a wind speed of 5m/s.
In order to further validate the approach, we computed the signal in channel 1 and 2 assuming a wind speed of 5 m/s and considering 3 optical thicknesses (0.1, 0.2 and 0.3 at 0.55 mm). The aerosol model used is a maritime (which is a good approximation in the middle of the ocean) and the ozone content is given by TOMS. As we can see Figures 7, the optical thickness of 0.1 fits the measurements in the two channels with a good agreement.

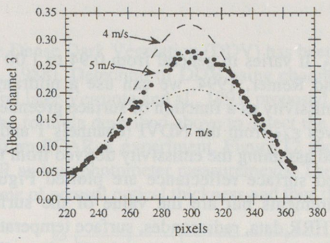

Figure 6: Plot of the surface reflectance in channel 3 over sunglint.
Also reported, comparisons with theoretical computations for several wind speed

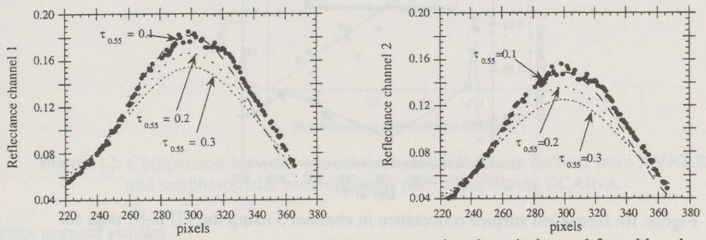

Figures 7: Retrieval of the aerosol optical thickness assuming the wind speed found by channel 3.

We performed the same procedure with the 4 other scenes. Figure 8 gives the results of the reflectance using a wind speed as deduced Figure 6. Figures 9 show the retrieved reflectances assuming a constant optical thickness for each scene. The good agreement between the computations and the measurements shows first the good retrieval of the reflectance in channel 3 and water vapor from T_4 and T_5. It also demonstrates that it is possible to retrieve aerosol optical thickness over the sunglint.

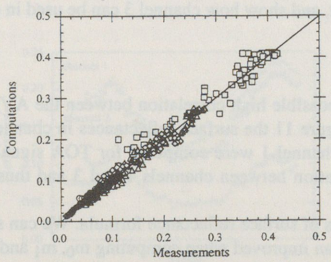

Figure 8: Comparisons for 5 scenes between retrieved reflectance
and computation using the wind speed.

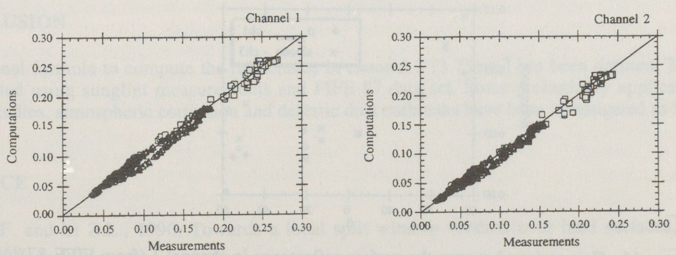

Figure 9: Comparisons for 5 scenes between measured and computed reflectance
assuming a constant aerosol optical thickness and wind speed for each scene.

3.3. Validation over land

Over land, we need the emissivity ε_{45}. It varies in general from 0.94 to 1.00 following the different kinds of target. As suggested by Kaufman and Remer, 1994, we can use a midrange emissivity of 0.97. Another assumption may be to represent the emissivity as a function of surface greenness following the formula of Van de Griend and Owe, 1993, which gives ε_{45} from the NDVI (channels 1 and 2). The formula of the surface reflectance in channel 3 has been tested assuming the emissivity derived from the NDVI and using the FIFE-87 data set. The results of the retrieved surface reflectance are plotted Figure 10 where the points called "Measurements" are not real measurements but are the value of the surface reflectance retrieved from MODTRAN simulations using all AVHRR data, radiosondes, surface temperature measurements. In this figure we compare our results with this given by the formula developed by Kaufman [Kaufman and Remer, 1994].

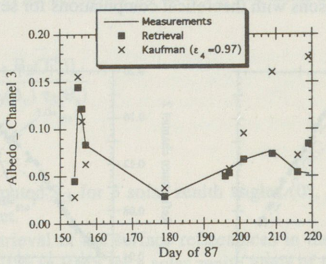

Figure 10: Retrieved surface reflectance in channel 3 using the FIFE-87 data set

5 - APPLICATIONS

In this part, we present some applications of the surface reflectance in channel 3 for specific studies. We first look at the advantage to use channel 3 for the surface properties retrieval. We use the formula to detect the Dense Dark Vegetation in channel 1 and to perform an aerosol optical thickness retrieval over these targets. At last we study a desertic aerosol event, and show how channel 3 can be used in desertic aerosol retrieval.

5.1. Surface properties retrieval.

Kaufman and Remer pointed out a possible high correlation between the AVHRR channels 1 and 3. Using the FIFE-87 data set, we compare in Figure 11 the surface reflectances in channels 1 and 3 versus the view zenith angle. The surface reflectances of channel 1 were computed for TOA signal using 6S [Vermote et al, 1994]. Figure 14 confirms the good correlation between channels 1 and 3 and thus shows the potentiality to BRDF studies using channel 3.
This figure also shows the limitations of surface reflectance formula. We can see a disagreement for view zenith angles greater than 50°, but that be can improved when computing m_0, m_1 and m_2 (equation 05). Currently, only angles from 0° to 50° has been used.

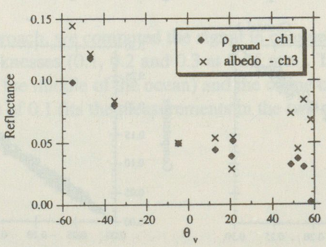

Figure 11: Comparison between the surface reflectance in channel 1 (from FIFE-87) and the surface reflectance in channel 3 (from eq 06).

5.2. Aerosol retrieval over land

The class of vegetation called the Dense Dark Vegetation (DDV) has been used to performed aerosols retrieval over land (Kaufman and Sendra, 1988). Detection of DDV using channel 3 brightness temperature has been assessed by Holben at al, 1991, and later Vermote and al., 1993, proposed to use the surface reflectance defined by Stowe et al., 1991. We tried the formula described above to detect the DDV and then to retrieve the aerosol optical thickness using the data from SCAR-A experiment. Figure 12 shows the comparisons between optical thicknesses derived from AVHRR and sunphotometer measurements. The agreement between the two is good, which confirms the retrieval scheme of aerosol optical thickness and thus the efficiency of dark surface detected.

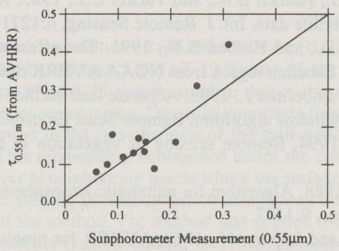

Figure 12: Comparison between optical thickness at 0.55 µm derived from AVHRR and sunphotometer measurements performed during SCAR-A.

5.3. Desertics aerosol studies

Dust outbreaks generation, transport and deposition are significant biospheric processes [Morales, 1979]. One of the important aspect of the desertic aerosol study is the estimate of the total mass of dust. Channel 3 centered at a longer wavelength should help in the retrieval of the size distribution which is critical in the mass estimate.
A preliminary study of an event of dust was performed using images taken over Dakar (Senegal) in 1988 [Jankowiak and Tanré, 1992]. A plot over a cloud of dust, Figure 13, shows very well that the reflectance in channel 3 can be used to identify dusty areas. Quantitative analysis is on going

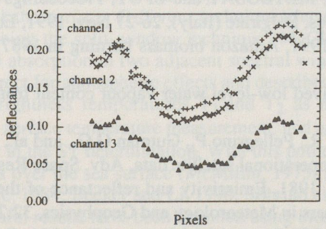

Figure 13: Plot of channel 1, 2 and 3 reflectances observed over a dust event in 1988 near Dakar.

6 - CONCLUSION

An operational formula to compute the reflectance in channel 3 (3.75mm) has been defined. This formula has been validated using sunglint measurements and FIFE-87 data set. Some preliminary applications to surface properties studies, atmospheric correction and desertic dust outbreaks have been investigated as further work.

REFERENCE

Becker F. and Li Z.L., 1990, Towards a local split window method over land surfaces, Int. J. Remote Sensing, 3:369.

Cox C. and Munk W., 1954, Measurement of the roughness of the sea surface from photographs of the sun's glitter, J. Opt. Soc. America, 44:838.

Dalu G., 1986, Satellite remote sensing of atmospheric water vapor, Int. J. Remote Sensing, 7:1089.

Daughtry C.S.T., Galio K.P., and Bauer M.E., 1983, Spectral estimates of solar radiation intercepted by corn canopies. Argon. J., 75:527.

Gatlin J.A., Sullivan R.J., and Tucker C.J., 1983, Monitoring global vegetation using NOAA AVHRR data, Proceedings of the IGAARS Symposium, San Francisco, California I, PF2, 7.1.

Holben B.N., Vermote E., Kaufman Y.J., Tanré D., and Kalb V., 1991, Aerosol retrieval over land from AVHRR data - Application for atmospheric correction, IEEE Trans. on Geosci. and Remote Sensing, 30:212.

Jankowiak I. and Tanré D., 1992, Satellite climatology of Saharan dust outbreaks: Method and preliminary results, J. of Climate, 5:646.

Justice C.O., Townshend J.R.G., Holben B.N., and Tucker C.J., 1985, Analysis of the phenology of global vegetation using meteorological satellite data, Int. J. Remote Sensing, 6:1271.

Justice C.O., Eck T.F., Tanré D., and Holben B.N., 1991, The effect of water vapour on the normalized difference vegetation index for the Sahelian region from NOAA AVHRR data, Int. J. Remote Sensing, 12:1165.

Kerr Y.H., Lagouarde J.P., and Imbernon J., 1992, Accurate land surface temperature retrieval from AVHRR data with use of an improved split window algorithm, Remote Sens. Environ., 41:197.

Kaufman Y.J. and Remer L. 1994, Remote sensing of vegetation in the mid-IR: the 3.75 µm channel, submitted to IJRS.

Kaufman Y.J. and Sendra C., 1988, Algorithm for automatic atmospheric corrections to visible and near-IR satellite imagery, Int. J. Remote Sens. 9:1357.

Malingreau, J.P., Tucker C.J., and Laporte N., 1989, AVHRR for monitoring global tropical deforestation, Int. J. Remote Sens., 10:855.

Mc Millin L.M., 1975, Estimation of sea surface temperature from two infrared window measurements with different absorption, J. geophys. Res., 80:5113.

Morales C., 1979, Saharan dust: Mobilization, Transport, Deposition. SCOPE Rep. 14. C . Morales, Ed., Swedish Natural Science Research Council, pp. 297.

Ottlé C. and Vidal-Madjar D., 1992, Estimation of Land surface temperature with NOAA 9 data, Remote Sens. Environ., 40:27.

Prabhakara C., Dalu G., and Kunde V.G., 1974, Estimation of sea surface temperature from remote sensing in the 11 to 13 µm window region, J. geophys. Res., 79:5039.

Rao, N.C.R., Stowe L.L., and McClain E.P., 1989, Remote sensing of aerosol over the ocean using AVHRR data. Theory, practice and application, Int. J. Remote Sensing, 10:743.

Seguin B., Fischer A, Kerdiles H., Louahala S., and Podaire A., 1992, Suivi agroclimatique des cultures en France à partir des données NOAA, METEOSAT and SPOT, Proceedings of the 2nd conference on remote sensing applied to agricultural statistics, Belgirate (Italy), 26-27 Nov. 1991, Ed. by JRC Ispra:339.

Setzer, A.W. and Pereira M.C., 1991, Amazon biomass burning in 1987 and their tropospheric emissions, Ambio, 20:19.

Schluessel P., 1989, Satellite derived low-level water vapour content from synergy of AVHRR with HIRS, Int. J. Remote Sensing, 10:705-721.

Stowe L.L., McClain E.P., Carey R., Pellegrino P., Gutman G.G., and al., 1991, Global distribution of cloud cover derived from NOAA/AVHRR operational satellite data, Adv. Space Res., 11:51.

Takashima T. and Takayama Y., 1981, Emissivity and reflectance of the model sea surface for the use of AVHRR data of NOAA satellite, Papers in Meteorology and Geophysics, 32:267.

Tucker C.J., Holben B.N. Elgin J.H. Jr., and McMurtrey J.E., 1981, Remote sensing of total dry matter accumulation in winter wheat. Remote Sensing Environ., 11:171.

Tucker C.J., Vanpraet C.L., Boerwinkel E., and Gaston A., 1983, Satellite remote sensing of total dry matter production in the Senegalese Sahel: 1980-1984, Remote Sens. Environ., 13:461.

Tucker C.J., Vanpraet C.L., Sharman M.J., and Van Ittersum G., 1985, Satellite remote sensing of total herbaceous biomass production in the Senegalese Sahel: 1980-1984, Remote Sens. Environ., 17:233.

Van de Griend and Owe A.A., 1993, On the relationship between thermal emissivity and normalized difference vegetation index for natural surfaces, Int. J. Remote Sens., 14:1119.

Vermote E., El Saleous N., and Holben B., 1993, Atmospheric correction of AVHRR visible and near infrared data. Proceedings of the workshop on atmospheric correction of Landsat Data, 21-25.

Vermote E., Tanré D., Herman M., and Morcrette J.J., 1994, Second simulation of the satellite signal in the solar spectrum: An overview, In preparation.